Long noncoding RNA *pncRNA-D* reduces cyclin D1 gene expression and arrests cell cycle through RNA m^{6}A modification

Received for publication, October 24, 2019, and in revised form, March 4, 2020 Published, Papers in Press, March 12, 2020, DOI 10.1074/jbc.RA119.011556

Ryoma Yoneda[‡], Naomi Ueda[‡], Kousuke Uranishi[§], Masataka Hirasaki[§], and Riki Kurokawa[‡1]

From the Divisions of [‡]Gene Structure and Function and [§]Developmental Biology, Research Center for Genomic Medicine, Saitama Medical University, Hidaka-shi, Saitama 350-1241, Japan

Edited by Ronald C. Wek

pncRNA-D* is an irradiation-induced 602-nt long noncoding RNA transcribed from the promoter region of the cyclin D1 (*CCND1*) gene. *CCND1* expression is predicted to be inhibited through an interplay between *pncRNA-D* and RNA-binding protein TLS/FUS. Because the *pncRNA-D*–TLS interaction is essential for *pncRNA-D*–stimulated *CCND1* inhibition, here we studied the possible role of RNA modification in this interaction in HeLa cells. We found that osmotic stress induces *pncRNA-D* by recruiting RNA polymerase II to its promoter. *pncRNA-D* was highly m^{6}A-methylated in control cells, but osmotic stress reduced the methylation and also arginine methylation of TLS in the nucleus. Knockdown of the m^{6}A modification enzyme methyltransferase-like 3 (METTL3) prolonged the half-life of *pncRNA-D*, and among the known m^{6}A recognition proteins, YTH domain-containing 1 (YTHDC1) was responsible for binding m^{6}A of *pncRNA-D*. Knockdown of METTL3 or YTHDC1 also enhanced the interaction of *pncRNA-D* with TLS, and results from RNA pulldown assays implicated YTHDC1 in the inhibitory effect on the TLS–*pncRNA-D* interaction. CRISPR/Cas9-mediated deletion of candidate m^{6}A site decreased the m^{6}A level in *pncRNA-D* and altered its interaction with the RNA-binding proteins. Of note, a reduction in the m^{6}A modification arrested the cell cycle at the G_0/G_1 phase, and *pncRNA-D* knockdown partially reversed this arrest. Moreover, *pncRNA-D* induction in HeLa cells significantly suppressed cell growth. Collectively, these findings suggest that m^{6}A modification of the long noncoding RNA *pncRNA-D* plays a role in the regulation of *CCND1* gene expression and cell cycle progression.

Long noncoding RNAs (lncRNAs)[2] are the class of RNA longer than 200 nt that do not code for proteins. They are involved in diverse mechanisms such as organ development, differentiation, circadian rhythm, and adipogenesis (1). lncRNAs are also related to cell cycle and cancer proliferation (2–5). We have previously discovered the lncRNA named *pncRNA-D* (promoter-associated ncRNA), which is transcribed from the promoter region of *CCND1* (cyclin D1) (6). *pncRNA-D* is an irradiation-induced 602-nt-long lncRNA that binds to RNA-binding protein TLS (translocated in liposarcoma)/FUS (fused in sarcoma), especially at the C-terminal RGG2–zinc finger–RGG3 domains (7, 8). The interplay with *pncRNA-D* changes the conformation of TLS, which enables it to bind CBP and inhibits its histone acetyltransferase activity at the *CCND1* promoter (6, 8). This *pncRNA-D*–TLS interaction is predicted to repress the expression of *CCND1* (6, 9). Because cyclin D1 is a key regulator of cell cycle at G_1/S phase checkpoint (10, 11), *pncRNA-D* is expected to be involved in the regulation of cell cycle.

Recently, RNA modifications have drawn great attention. More than a hundred RNA modifications including methylation, acetylation, phosphorylation, and ubiquitylation occur in various RNAs such as mRNA, tRNA, and in lncRNAs (12, 13). One of the most abundant modifications is N^6-methyladenosine (m^{6}A) methylation, which is found in both mRNAs and lncRNAs (14, 15). m^{6}A methylation is modified by a protein complex that consists of METTL3 (methyltransferase-like 3), METTL14, and WTAP (Wilm's tumor protein) (16–18) and is likely to occur in the motif of RRACH (R; A or G, H; except for G). This modification is reversible, because demethylases such as FTO (fat mass and obesity-associated) and ALKBH5 (alkB homolog 5) are also discovered (19, 20).

YTH domain–containing proteins and hnRNPs are the main recognition proteins of the m^{6}A modification (21, 22). YTHDF1 and YTHDF2 recognize this modification in the cytoplasm and have roles in translational regulation and RNA stability, respectively (23–26). In the nucleus, YTHDC1, hnRNP A2B1, and hnRNP C are responsible for m^{6}A recognition (27–29). Although the function of hnRNP A2B1 is not clear, hnRNP C is reported to change secondary structure of mRNA, and YTHDC1 regulates RNA splicing.

m^{6}A modifications are broadly involved in diseases such as cancer, obesity, diabetes, and infertility (30). It is also related to controlling circadian rhythm and X chromosome inactivation

This work was supported by MEXT/JSPS KAKENHI Grants Wakate (B) 17K18065 (to R. Y.) and Kiban (C) 18K06939 (to R. K.). The authors declare that they have no conflicts of interest with the contents of this article.

This article contains Fig. S1.

[1] To whom correspondence should be addressed: Division of Gene Structure and Function, Research Center for Genomic Medicine, Saitama Medical University, 1397-1 Yamane, Hidaka-shi, Saitama 350-1241, Japan. Tel.: 81-42-984-0389; Fax: 81-42-984-0398 E-mail: rkurokaw@saitama-med.ac.jp.

[2] The abbreviations used are: lncRNA, long noncoding RNA; DSB, double-stranded break; DGCR, DiGeorge critical region; GST, glutathione *S*-transferase; hnRNP, heterogeneous nuclear ribonucleoprotein; METTL, methyltransferase like; NE, nuclear extract; RIP, RNA immunoprecipitation; qPCR, quantitative PCR; m^{6}A, N^6-methyladenosine; KO, knockout; GTF, general transcription factor; Pol, polymerase; TBP, TATA-binding protein; TFIIB, transcription factor IIB; strep, streptomycin; PS, penicillin/streptomycin; nt, nucleotide(s); FBS, fetal bovine serum.

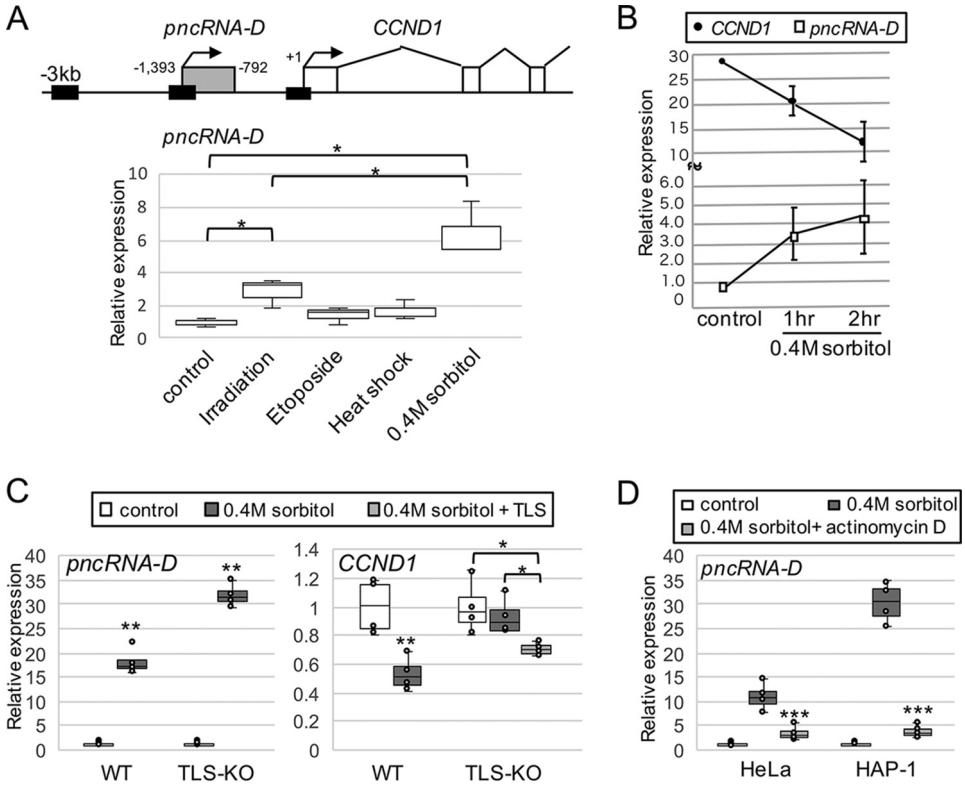

Figure 1. Expression of *pncRNA-D* is enhanced after osmotic stress, and TLS is essential for *CCND1* repression by *pncRNA-D*. *A*, schematic drawing of *CCND1* upstream region (*top*) and relative expression level of *pncRNA-D* in HeLa cell after indicated stimuli was detected by RT-qPCR (*bottom*). Expression levels in control cells were set to a value of 1.0 ($n = 3$). *Black boxes* in the schematic drawing indicate the regions examined in Fig. 2*B*. *B*, relative expression level (normalized to *GAPDH*) of *CCND1* and *pncRNA-D* was evaluated by RT-qPCR. Expression level of *pncRNA-D* in control cells was set to a value of 1.0 ($n = 5$). *C*, relative expression level (normalized to *GAPDH*) of *pncRNA-D* (*left panel*) and *CCND1* (*right panel*) of WT and TLS-KO HAP1 cells before and after sorbitol treatment. For TLS-KO HAP-1 cells, GFP-tagged TLS was overexpressed at the same time with sorbitol treatment (*light gray box*). Expression levels in control cells were set to a value of 1.0 ($n = 4$). *D*, relative expression level (normalized to *GAPDH*) of *pncRNA-D* after 0.4 M sorbitol treatment with or without actinomycin D treatment. Expression levels in control cells were set to a value of 1.0 ($n = 5$). *, $p < 0.05$; **, $p < 0.01$.

(31, 32). Several studies have reported the involvement of m^{6}A modification in the cell cycle as well. Knockdown of FTO delays cell cycle at the entry of G_2 phase in adipogenesis (33), and knockdown of METTL3 results in cell cycle arrest at G_0/G_1 phase (34). Moreover, WTAP participates in cell cycle progression by stabilizing cyclin A2 mRNA (35), and knockdown of YTHDC1 reduces HeLa cell proliferation (36). However, despite diverse comprehensive studies of m^{6}A modification, there are very few reports that discovered the function of m^{6}A modification in individual RNA, especially in lncRNAs.

In this study, we demonstrated that *pncRNA-D* was induced after osmotic stress by recruitment of RNA polymerase II to its promoter. We also confirmed that TLS was required for repression of *CCND1* expression. Moreover, *pncRNA-D* was highly m^{6}A-methylated in the usual state, but its level decreased after exposure to cellular stresses. m^{6}A methylation of *pncRNA-D* was preferentially recognized by nuclear RNA-binding protein, YTHDC1. The m^{6}A modification of *pncRNA-D* shortened its life time, and YTHDC1 blocked the interaction with TLS. In addition, knockdown of *pncRNA-D* successfully rescued the cell cycle arrest at the G_0/G_1 phase caused by reduced m^{6}A methylation. In conclusion, we elucidated the importance of *pncRNA-D* and TLS in the inhibition of *CCND1*, and this inhibition is due to increased expression and decreased RNA m^{6}A modification of *pncRNA-D*.

Results

Osmotic stress induces pncRNA-D by recruiting general transcription factor proteins to the promoter region

Because *pncRNA-D* is induced by irradiation (6), we tested whether other stimuli could also induce *pncRNA-D*. HeLa cells were treated with heat shock, osmotic stress, or etoposide, which induce DNA double-stranded break. A double-stranded break was detected by γH2AX antibody, but no difference was observed among the stimuli tested compared with irradiation (Fig. S1*A*). Although heat shock and etoposide treatment showed slight increase of *pncRNA-D*, only osmotic stress by 0.4 M sorbitol treatment significantly induced *pncRNA-D* other than irradiation (Fig. 1*A*, *bottom panel*). Therefore, in terms of convenience and induction efficiency compared with irradiation, we decided to employ osmotic stress instead of irradiation in this study. HeLa cells were treated with 0.4 M sorbitol, and the expression levels of *pncRNA-D* and *CCND1* were examined at 2 and 3 h after treatment. As a result, negative correlation between *pncRNA-D* and *CCND1* expression was observed (Fig. 1*B*).

We then validated the importance of TLS in the *pncRNA-D* provoked *CCND1* repression system. WT HAP1 cells and TLS-knockout (KO) HAP1 cells were treated with 0.4 M sorbitol and increased expression of *pncRNA-D* was detected in both cells

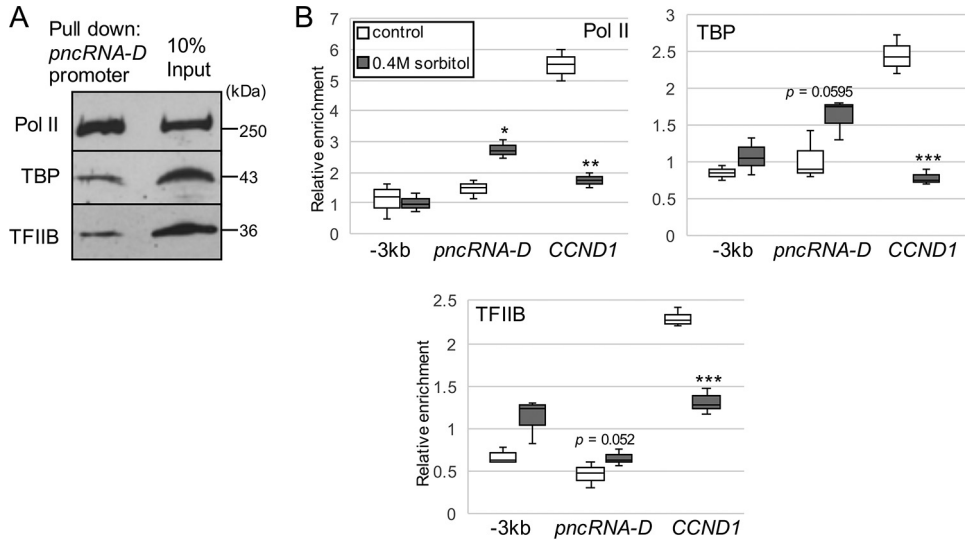

Figure 2. General transcription factors are recruited to *pncRNA-D* promoter after osmotic stress. *A*, Western blotting analysis was conducted after pulldown assay using biotinylated *pncRNA-D* promoter with HeLa nuclear extract. Interaction with RNA Pol II, TBP, and TFIIB was examined by Western blotting analysis. *B*, ChIP assay by antibody against Pol II, TBP, and TFIIB at three regions indicated by *black boxes* in Fig. 1*A*. Enrichment of each protein was compared before and after osmotic stress ($n = 3$). *, $p < 0.05$; **, $p < 0.01$; ***, $p < 0.005$.

(Fig. 1*C*, *left panel*). On the other hand, *CCND1* expression was dropped to 50% after osmotic stress in WT cells, but not in the TLS-KO cells (Fig. 1*C*, *right panel*). To observe whether the overexpression of TLS in TLS-KO cells could rescue the repression of *CCND1*, GFP-tagged TLS overexpression vector was transfected to the TLS-KO cells. This resulted in the decrease of *CCND1* expression after osmotic stress (Fig. 1*C*, *right panel*, *light gray box*). These data confirmed the necessity of TLS in the *CCND1* repression mechanism.

To address whether the increased expression level of *pncRNA-D* by osmotic stress was due to enhanced expression and/or RNA stability, HeLa cells were treated with actinomycin D to stop the nascent transcription. The expression level of *pncRNA-D* was measured 2 h after actinomycin D treatment, but we could not detect dramatic increase in the expression even after sorbitol treatment (Fig. 1*D*).

Because lncRNAs are transcribed by general transcription factors (GTFs) like mRNAs (37), we searched for TATA-binding box around the *pncRNA-D* transcriptional start site but could not find any typical sequences. However, pulldown assay with biotinylated *pncRNA-D* promoter region incubated with HeLa nuclear extract (NE) successfully exhibited that GTFs could bind *pncRNA-D* promoter (Fig. 2*A*). Thus, the enrichment of GTFs were examined before and after osmotic stress. The enrichment of RNA polymerase II (Pol II), TATA-binding protein (TBP), and transcription factor IIB (TFIIB) was decreased at *CCND1* promoter after the stress (Fig. 2*B*). In contrast to *CCND1* promoter, the enrichment of Pol II increased after osmotic stress at *pncRNA-D* promoter (Fig. 2*B*). Although they were not significant, the recruitments of TBP and TFIIB to *pncRNA-D* promoter tended to increase after the stress. Taken together with the result of actinomycin D treatment, increased expression level of *pncRNA-D* after osmotic stress is caused by activated transcription caused by recruitment of GTFs to *pncRNA-D* promoter.

pncRNA-D is highly m^{6}A-modified, and this methylation destabilizes pncRNA-D

Because the interplay with TLS is a pivotal step for *CCND1* repression by *pncRNA-D*, we speculated that the interaction was influenced by the osmotic stress. RNA immunoprecipitation (RIP) assay was performed using antibody against TLS and HeLa cells with or without osmotic stress. As a result, the interaction between *pncRNA-D* and TLS was increased by 2-fold after the stress (Fig. 3*A*). In contrast to the enhanced expression level of *pncRNA-D* by osmotic stress, the amount of TLS in the nucleus was decreased after the treatment (Fig. 3*B*). TLS is known to change localization to cytoplasmic stress granules after sorbitol treatment (38), and we also confirmed the change in localization. We further quantified the alteration of arginine methylation of TLS and detected a slight decrease after the stress (Fig. 3*B*). This was in good agreement with our previous finding that arginine methylation of TLS blocks RNA binding (8).

Then we assumed that modification in *pncRNA-D* might also be influenced by osmotic stress and examined m^{6}A modification, which is one of the most abundant RNA modifications that occurs in mRNA and in lncRNA. According to the meRIP-seq data obtained from the NCBI's Gene Expression Omnibus database, transcripts from *CCND1* promoter are likely to be modified with m^{6}A, including the region of *pncRNA-D* (Fig. S1*B*). RIP assay with anti-m^{6}A antibody confirmed that *pncRNA-D* was highly methylated in normal condition, but its methylation dramatically decreased after osmotic stress or irradiation (Fig. 3*C*). We speculated on the cause of the decrease in *pncRNA-D* m^{6}A modification and measured expression levels of m^{6}A related proteins after osmotic stress or irradiation. As a result, WTAP, a component of m^{6}A modification complex, was halved by both treatments, but other proteins did not show much difference or had different effects among the two treatments (Fig. S1*C*), at least in mRNA level. Therefore, we assume

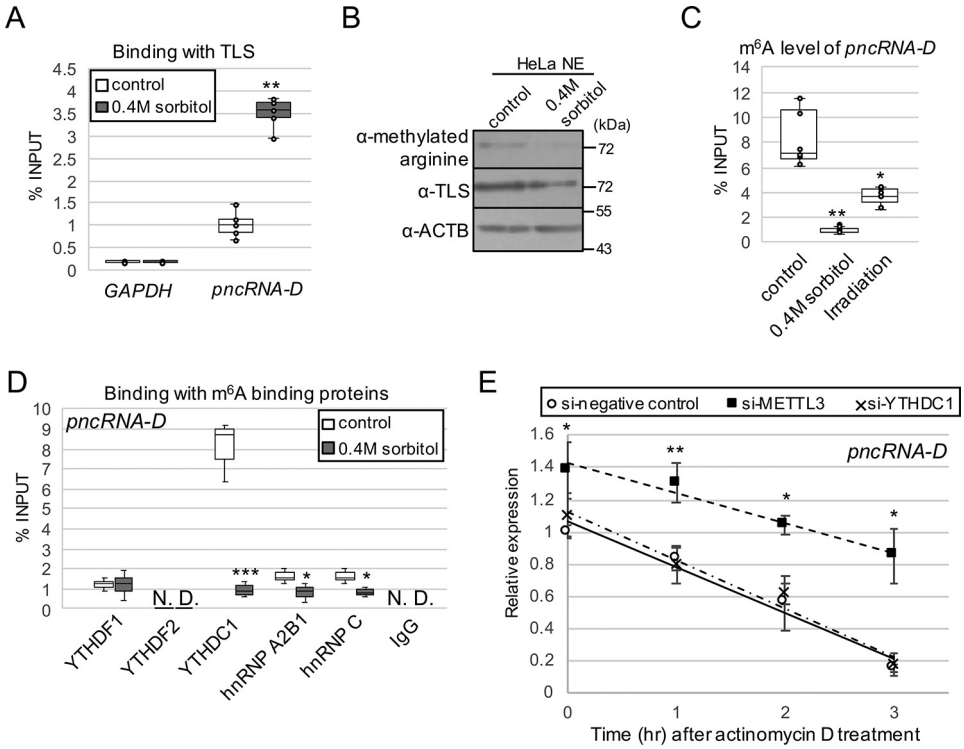

Figure 3. *pncRNA-D* is highly m^{6}A-modified, and the modification destabilizes *pncRNA-D*. *A*, the interaction between *pncRNA-D* and TLS was detected by RIP assay using TLS antibody with HeLa cells before and after osmotic stress ($n = 5$). *B*, Western blotting analysis using HeLa NE with or without 0.4 M sorbitol treatment. The arginine-methylated TLS level was compared with the total TLS level. ACTB was used as a loading control. A representative image of three independent experiments is shown. *C*, RIP assay with HeLa cell after osmotic stress or irradiation by m^{6}A antibody ($n = 5$). *D*, RIP assay as in *A* with indicated antibodies of m^{6}A recognition proteins. *pncRNA-D* bound to each recognition protein was measured by RT-qPCR ($n = 3$). *E*, relative expression level (normalized to *GAPDH*) of *pncRNA-D* after actinomycin D treatment with HeLa cells treated with siRNAs of negative control, METTL3, or YTHDC1. Expression levels at 1, 2, and 3 h after actinomycin D treatment are shown. Expression levels at 0 h in control cells were set to a value of 1.0 ($n = 5$). *, $p < 0.05$; **, $p < 0.01$; ***, $p < 0.005$.

that the decrease in *pncRNA-D* m^{6}A modification is caused by a reduced expression level of WTAP.

Next, we asked which of the m^{6}A-binding protein(s) recognize the m^{6}A modification of *pncRNA-D*. m^{6}A modification is recognized by YTHDF1 or YTHDF2 in the cytoplasm and YTHDC1, hnRNP A2B1, or hnRNP C in the nucleus. RIP assay with antibodies against the above five proteins revealed that YTHDF1, YTHDC1, hnRNP A2B1, and hnRNP C exhibited interaction with *pncRNA-D* (Fig. 3*D*). Unexpectedly, the cytoplasmic YTHDF1 was able to bind *pncRNA-D*. This is because despite predominant nuclear localization of *pncRNA-D*, a small portion of them localize in the cytoplasm. However, we focused on YTHDC1, which bound more intensely than other m^{6}A recognition proteins.

The major role of RNA m^{6}A methylation is to influence the stability of RNA (39, 40). Therefore, we tested whether the modification could affect the stability of *pncRNA-D* by knockdown of METTL3, a m^{6}A modification protein, or YTHDC1. Knockdown efficiency of METTL3 or YTHDC1 by siRNAs were detected by Western blotting analysis, and their protein levels decreased dramatically after 48 h (Fig. S1*D*). As a result of actinomycin D treatment, the expression level of *pncRNA-D* in the control HeLa cells reduced down to 50% in approximately 2 h, but the knockdown of METTL3 increased stability of *pncRNA-D* (Fig. 3*E*). Meanwhile, knockdown of YTHDC1 had no effect on *pncRNA-D* stability. Collectively, m^{6}A modification itself destabilizes *pncRNA-D*, but YTHDC1 is not involved in destabilization directly.

m^{6}A modification also interrupts the interaction between pncRNA-D and TLS

Because YTHDC1 did not influence the stability of *pncRNA-D*, we expected that YTHDC1 and m^{6}A modification have some other functions; thus, we examined the effect on the interaction between *pncRNA-D* and TLS. RIP assay by TLS antibody after knockdown of METTL3 or YTHDC1 resulted in increased interaction between TLS and *pncRNA-D* by ~2-fold (Fig. 4*A*). The result indicated that m^{6}A modification and YTHDC1 interrupts the binding between *pncRNA-D* and TLS.

To determine which adenosine residue(s) of *pncRNA-D* has m^{6}A modification, we searched for RRACH motif in the *pncRNA-D* sequence and found 12 motifs (Fig. S1*B*, *blue* and *red boxes*). m^{6}A modification especially tends to occur in the consensus sequence GGACU (41–44), and among the 602 nt of the full-length *pncRNA-D*, we could only find one motif at 465–469 nt (Fig. 4*B*, *top panel*, *gray box*). Notably, we previously identified that the sequence around GGACU of *pncRNA-D* strongly bound to RGG2-ZF-RGG3 domains of TLS, which were responsible for RNA binding (Fig. 4*B*, *middle panel*) (9). The meRIP-seq data also implied that m^{6}A modification occurs at the region around 3′ end of *pncRNA-D* (Fig. S1*B*); therefore we predicted that the GGACU motif at 465–469 nt is m^{6}A-

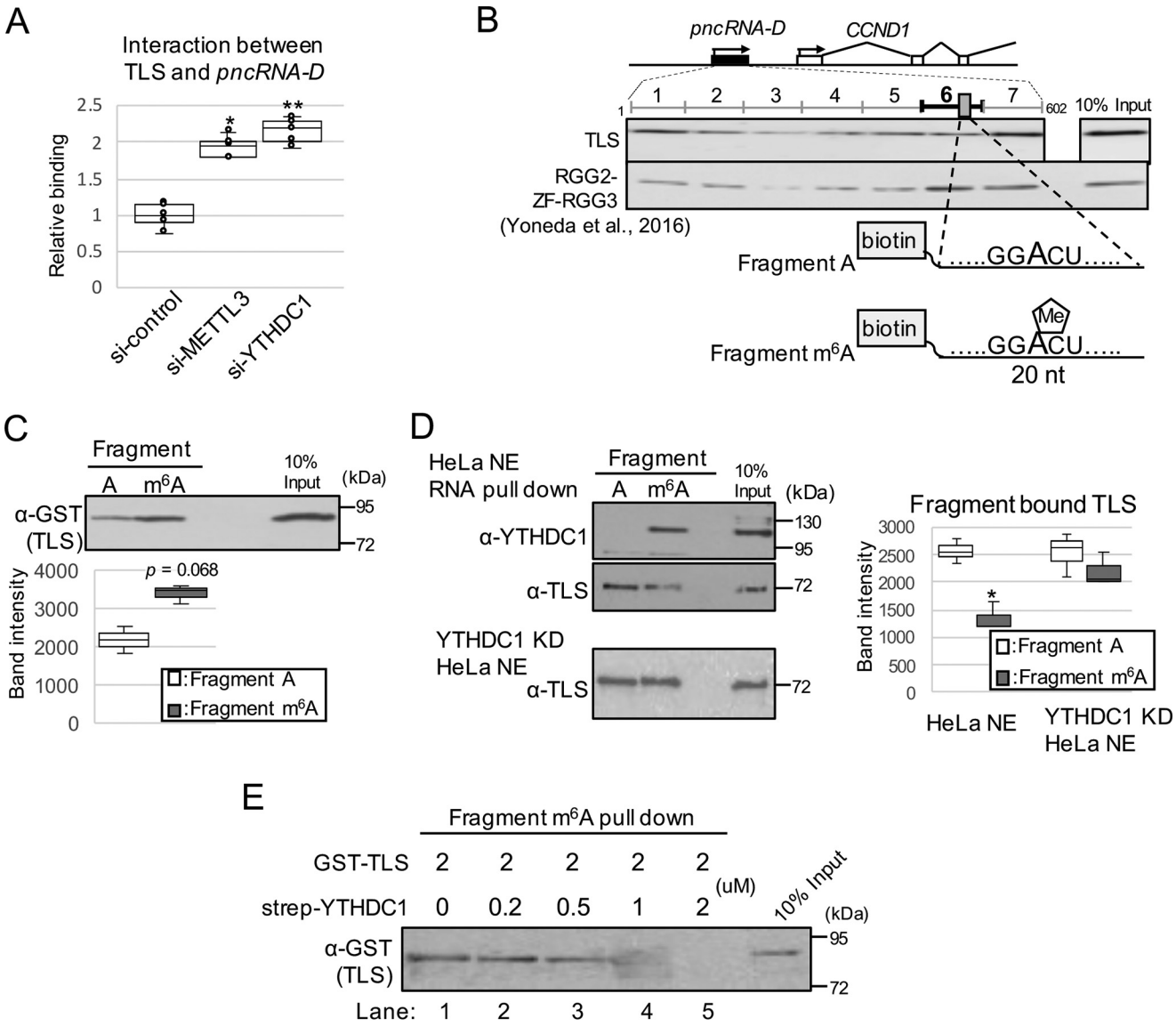

Figure 4. m^{6}A modification inhibits interaction between *pncRNA-D* and TLS by competitive binding of YTHDC1. *A*, RIP assay by TLS antibody with HeLa cells treated with siRNAs of negative control, METTL3, or YTHDC1 ($n = 5$). *, $p < 0.05$; **, $p < 0.01$. *B*, schematic drawing of full-length *pncRNA-D* and position of GGACU. The results of Western blotting analysis after RNA pulldown assay were cited from our previous paper in 2016 (9). 20-nt biotinylated fragment around GGACU was generated with (fragment m^{6}A) or without (fragment A) m^{6}A modification. *C* and *D*, RNA pulldown assay using fragment A or m^{6}A incubated with GST–TLS (*C*) or HeLa nuclear extract (*D*). RNA-bound proteins were detected by the indicated antibodies. Representative images of three individual experiments are shown. The band intensity of TLS bound to fragment A or fragment m^{6}A in HeLa NE or YTHDC1 KD HeLa NE was quantified by ImageJ (RRID:SCR_003070) (*D*, *right*) ($n = 3$); *, $p < 0.05$. *E*, RNA pulldown assay using fragment m^{6}A incubated with GST–TLS and various concentration of strep-YTHDC1. Fragment m^{6}A was incubated with GST–TLS and strep-YTHDC1 at the indicated amount, and the RNA bound GST–TLS was detected by Western blotting analysis.

modified and might play an important role in TLS–*pncRNA-D* interaction. To determine the effect of m^{6}A modification at the site, we generated a 20-nt biotinylated RNA fragment around GGACU with or without m^{6}A modification (fragment m^{6}A and fragment A, respectively; Fig. 4*B*, *bottom panel*). Unpredictably, although it was not significant, RNA pulldown assay with GST-tagged TLS showed stronger binding with fragment m^{6}A than fragment A (Fig. 4*C*).

We further investigated the effect of m^{6}A modification on *pncRNA-D* and TLS interaction using HeLa NE. RNA pulldown assay with fragment m^{6}A or fragment A was conducted with HeLa NE, and as expected, endogenous YTHDC1 bound to fragment m^{6}A but not to nonmethylated fragment A (Fig. 4*D*, *top panel*). On the other hand, TLS in HeLa NE bound strongly to fragment A compared with fragment m^{6}A (Fig. 4*D*, *middle panel*), which conflicts with the data of *in vitro* assay (Fig. 4*C*). We anticipated that YTHDC1 in the HeLa NE might block the interaction between TLS and fragment m^{6}A. To test this hypothesis, NE was prepared from YTHDC1 knockdown HeLa cells, and the same experiment was conducted. As a result, TLS bound to fragment m^{6}A at a comparable level with fragment A (Fig. 4*D*, *bottom panel*), exhibiting the competitive effect of YTHDC1 on TLS–*pncRNA-D* interplay.

Next, we evaluated the inhibitory effect of YTHDC1 on interaction between fragment m^{6}A and TLS using *Escherichia coli*.

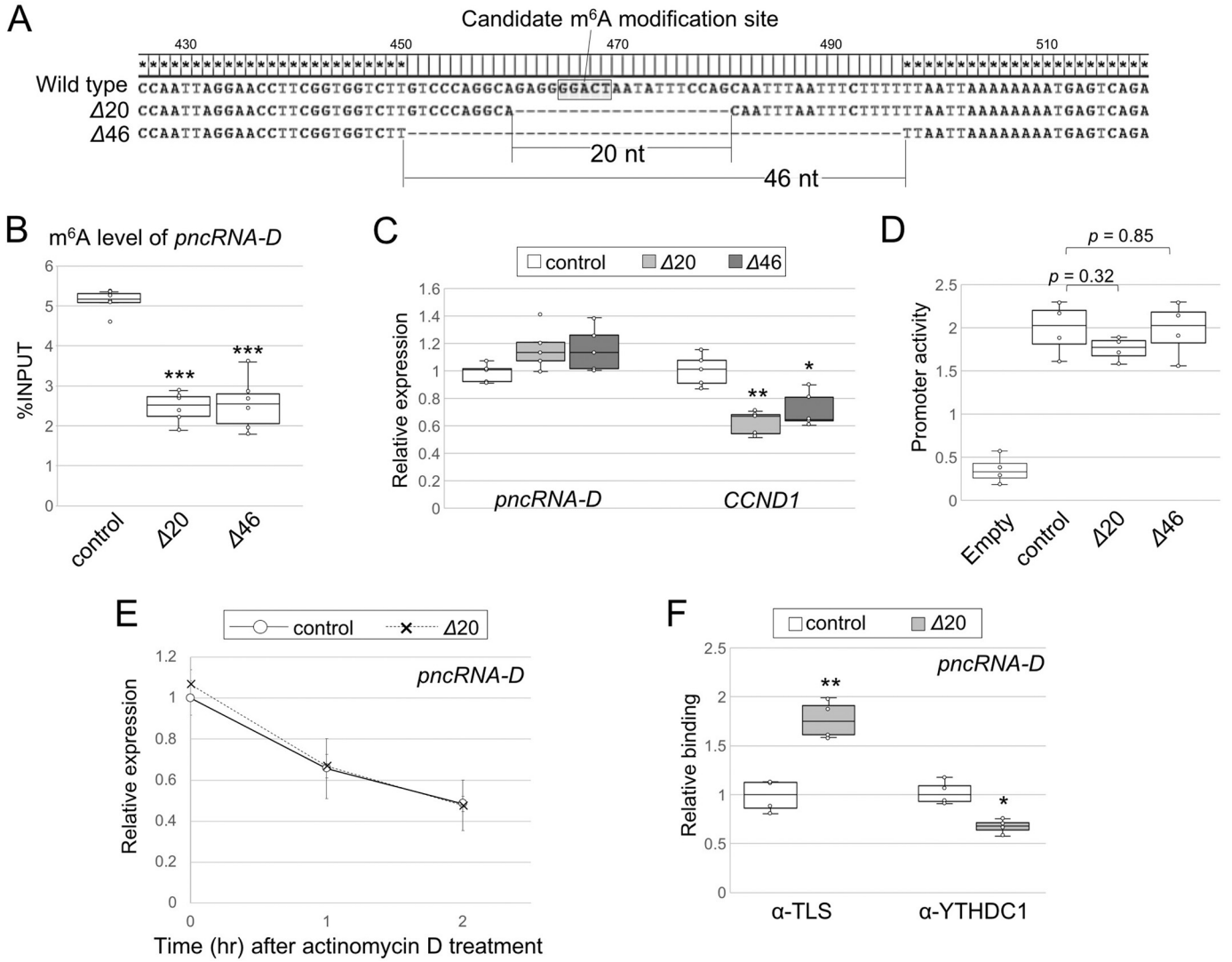

Figure 5. Deletion of GGACU motif in *pncRNA-D* decreases m^{6}A modification level and alters interaction with RNA-binding proteins, but not RNA stability. *A*, sequences deleted by CRISPR/Cas9 are described. HAP1 clones named Δ20 and Δ46 lack 20 and 46 nucleotides around GGACT, respectively. *B*, RIP assay with WT or GGACT deleted HAP1 cells by anti-m^{6}A antibody ($n = 5$). *C*, relative expression level (normalized to *GAPDH*) of *pncRNA-D* and *CCND1* of WT or GGACT-deleted HAP1. Expression levels in control cells were set to a value of 1.0 ($n = 5$). *D*, luciferase reporter assay with control or GGACT deleted promoter region of *CCND1* ($n = 4$). *E*, relative expression level (normalized to *GAPDH*) of *pncRNA-D* after actinomycin D treatment in WT or GGACT deleted HAP1. Expression levels of 1 and 2 h after actinomycin D treatment are shown. Expression levels at 0 h in control cells were set to a value of 1.0. *F*, RIP assay as in *B* with antibodies against TLS or YTHDC1. *pncRNA-D* bound to each protein was measured by RT-qPCR ($n = 4$). *, $p < 0.05$; **, $p < 0.01$; ***, $p < 0.005$ in all the figures.

overexpressed strep-YTHDC1. strep-YTHDC1 was incubated with fragment A or fragment m^{6}A, and RNA pulldown assay confirmed that it preferentially bound to fragment m^{6}A (Fig. S1*E*), which resembles the characteristic of endogenous YTHDC1. Then various concentration of strep-YTHDC1 were incubated with GST–TLS and fragment m^{6}A. We observed decreased interaction of GST–TLS with fragment m^{6}A from the strep-YTHDC1 concentration at one-fourth of GST–TLS (Fig. 4*E*, *lane 3*). By incubating same concentration of GST–TLS and strep-YTHDC1, GST–TLS was not able to bind fragment m^{6}A at all (Fig. 4*E*, *lane 5*). Collectively, YTHDC1 binds to m^{6}A-methylated *pncRNA-D* and inhibits the interaction between *pncRNA-D* and TLS.

To confirm the importance of GGACU motif of *pncRNA-D*, we removed the sequence around the motif with the CRISPR/Cas9 system. HAP1 cells were selected for the assay, because they are haploid cells, and the *CCND1* inhibitory system by TLS and *pncRNA-D* works in these cells as demonstrated in Fig. 1. We obtained two clones that lack the GGACU motif with a 20- or 46-nt deletion, named Δ20 or Δ46, respectively (Fig. 5*A*). According to the results of the RIP assay, the m^{6}A modification level was halved in both Δ20 and Δ46 cells (Fig. 5*B*). The expression level of *pncRNA-D* was slightly higher in mutated cells, and that of *CCND1* was ~60% of the WT (Fig. 5*C*). Luciferase reporter assay was conducted to validate the effect of deleted genomic regions on promoter activity. As a result, the sequence deleted in Δ20 or Δ46 cells had no significant effect on *CCND1* promoter activity (Fig. 5*D*), suggesting the reduced *CCND1* expression was due to transcripts lacking GGACU motif but not the deleted genomic sequences. Because Δ20 cells had shorter deletion, we further analyzed Δ20 cells for elucidating the function of the *pncRNA-D* GGACU motif.

Reduced m^{6}A modification level stabilized *pncRNA-D* and altered interaction with RNA-binding proteins in HeLa cells (Figs. 3 and 4); therefore we inquired whether deletion of GGACU motif affect the stability and/or the interactions. Actinomycin D was treated to WT and Δ20 HAP1 cells, but the amount of *pncRNA-D* decreased similarly in both cells (Fig. 5*E*). Next, the binding between *pncRNA-D* with TLS or YTHDC1 was detected in WT or Δ20 cells. The results clearly showed that GGACU deletion enhanced the binding with TLS by 1.8-fold and reduced the interaction with YTHDC1 (Fig. 5*F*), which supports the YTHDC1 inhibitory effect observed in Fig. 4. The above results apparently indicate the GGACU motif at positions 465–469 of *pncRNA-D* is m^{6}A-modified and responsible for TLS and YTHDC1 binding but not stabilization.

pncRNA-D is involved in the normal cell cycle

Finally, we considered the participation of *pncRNA-D* and m^{6}A modification in cell cycle and cell proliferation. HeLa cells were fractionated into G_0/G_1, S, and G_2/M phase cells according to the amount of DNA by FACS (Fig. 6*A*, *top panel*). Expression levels of *pncRNA-D* and *CCND1* were measured by RT-qPCR in each fraction, and again negative correlation between *pncRNA-D* and *CCND1* was observed (Fig. 6*A*, *bottom panel*) as in response to the osmotic stress (Fig. 1*B*). These data raised the possibility that *pncRNA-D* is also involved in normal cell cycle, not only in response to cellular stresses.

HeLa cells were treated with siRNAs of *pncRNA-D*, METTL3, or YTHDC1 to investigate the effect of *pncRNA-D* and RNA methylation on cell cycle. By knockdown of *pncRNA-D*, we detected a slight increase in the population of S phase cells compared with control HeLa cells, although it was not significant (Fig. 6, *B* and *C*). Knockdown of METTL3 was implicated to arrest cell cycle at G_0/G_1 phase (34), and we also validated that si-METTL3 increased cell population of G_0/G_1 phase and loss of G_2/M phase peak (Fig. 6, *B* and *C*). A similar effect was observed by knockdown of YTHDC1 (Fig. 6, *B* and *C*). In addition to the above effects, osmotic stress also increased the population of the G_0/G_1 phase and abolished the G_2/M phase peak (Fig. 6, *B* and *D*). Moreover, we evaluated the effect of *pncRNA-D* knockdown at the same time with the above treatments. As a result, double knockdown of METTL3 or YTHDC1 with *pncRNA-D* partially rescued the G_0/G_1 phase cell cycle arrest (Fig. 6*C*) and exhibited recovery of G_2/M phase peak (Fig. 6*B*). On the other hand, *pncRNA-D* knockdown in the osmotic stress–treated HeLa cells showed a slight shift of G_0/G_1 peak (Fig. 6*B*) but had no significant effect (Fig. 6*D*).

Additionally, the expression level of *CCND1* was measured after knockdown of METTL3, YTHDC1, and/or *pncRNA-D*. Knockdown of *pncRNA-D* increased *CCND1* expression level by 2-fold, and the knockdown of METTL3 or YTHDC1 dramatically decreased its expression (Fig. 6*E*). Notably, the expression of *CCND1* was recovered to control level by double knockdown of METTL3 or YTHDC1 with *pncRNA-D*. Taken together, *pncRNA-D* without m^{6}A or YTHDC1 reduces *CCND1* expression and subsequently arrest cell cycle.

Cell proliferation assay revealed that knockdown of *pncRNA-D* modestly promoted cell growth, although it was not significant (Fig. 7*A*). Knockdown of METTL3 or YTHDC1 reduced HeLa cell growth and by knockdown of *pncRNA-D* at the same time rescued the growth to some extent (Fig. 7*A*). HAP1 lacking GGACU motif (Δ20) proliferated slower compared with control cells (Fig. 7*B*), supporting the importance of m^{6}A modification of this motif in cell proliferation. Furthermore, the growth was delayed by inducing full-length *pncRNA-D* into HeLa cells, but the antisense *pncRNA-D* did not show such suppression (Fig. 7*C*). In conclusion, *pncRNA-D* is also involved in ordinary cell cycle and proliferation through m^{6}A modification.

Discussion

In this study, we demonstrate that lncRNA designated as *pncRNA-D* could be induced by osmotic stress and reduces expression of *CCND1* by interacting with RNA-binding protein, TLS. *pncRNA-D* is highly modified by m^{6}A in the usual state, but its level dramatically decreases after osmotic stress or irradiation. This methylation of *pncRNA-D* has effect on its stability and interaction with TLS. m^{6}A modification of *pncRNA-D* is recognized by nuclear YTHDC1, and this binding prohibits the interaction between *pncRNA-D* and TLS. Moreover, reduced RNA methylation level leads to cell cycle arrest, and *pncRNA-D* knockdown successfully rescues this arrest. In summary, we propose a model in which *pncRNA-D* inhibits the expression of *CCND1* via RNA methylation alteration and subsequently arrests the cell cycle (Fig. 7*D*).

Osmotic stress is not a very popular treatment, but it is one of the cellular stresses that induces ncRNAs. DoGs (downstream of genes) are a type of ncRNAs induced by osmotic stress and are transcribed from the 3′ regions of many coding genes (45). In addition, osmotic stress could alter gene expression of coding and noncoding genes (46). Osmotic stress and irradiation caused a similar level of DNA double-stranded break (DSB), and hence, we postulated that signaling cascade activated by DNA DSB might recruit general transcription factors to the *pncRNA-D* promoter. One candidate is signaling pathway activated by ATM/ATR. ATM is activated by DNA DSB, causes cell cycle arrest at G_1 or G_2, and activates DNA-repairing and stress-responsive genes. The signaling cascade downstream of ATM/ATR includes p53 and p21, of which responsible for G_1 cell cycle arrest (47, 48), which we observed by osmotic stress and METTL3 or YTHDC1 knockdown.

pncRNA-D is not the only lncRNA induced by irradiation or osmotic stress at the *CCND1* promoter, but there are several other lncRNAs induced by cellular stresses (*e.g. pncRNA-A*, *-B*, and *-E*) (6). This study only focused on *pncRNA-D* because it showed the highest induction level after irradiation among the *pncRNA*s, but there is a possibility that *pncRNA*s work coordinately to inhibit *CCND1* expression. In fact, other group has reported that *pncRNA-B*, which is transcribed just before transcriptional initiation site of *CCND1*, is highly expressed in Ewing Sarcoma patients (49). This lncRNA also negatively regulates the expression of *CCND1* and is involved in cell proliferation of Ewing sarcoma cell lines.

meRIP-seq data analysis and motif search indicated that the adenosine residue in the GGACU motif at nt 465–469 of *pncRNA-D* is likely to be methylated. The fact that most of the m^{6}A modifications in mRNAs and several ncRNAs occur

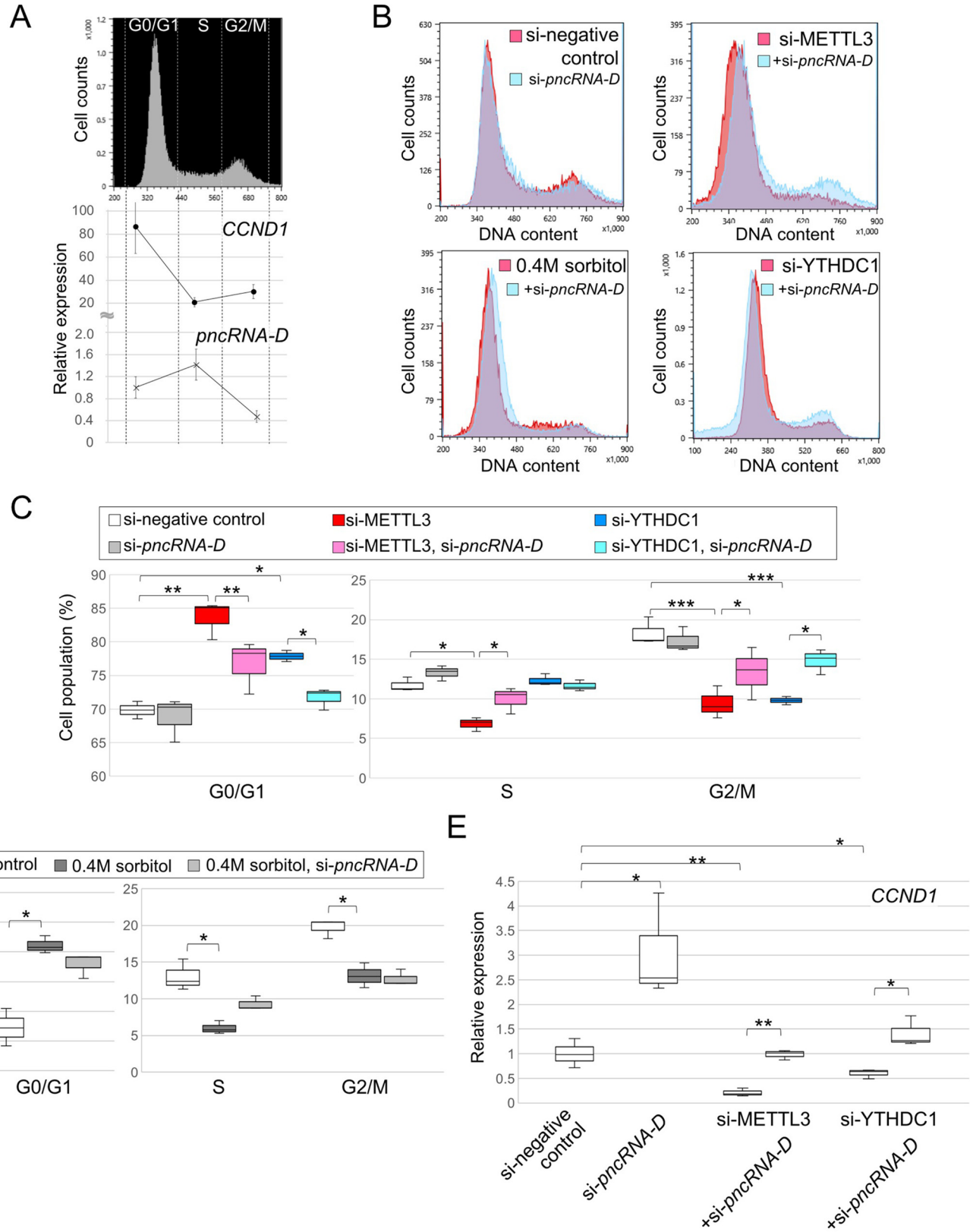

Figure 6. *pncRNA-D* rescues cell cycle arrest caused by decreased m^{6}A modification level. *A*, HeLa cells were sorted into G_0/G_1, S, and G_2/M phase cells by FACS (*top panel*), and the expression level of *CCND1* and *pncRNA-D* was measured in each fraction (*bottom panel*). The expression level of *pncRNA-D* in G_0/G_1 phase control cells was set to a value of 1.0 ($n = 5$). *B*, histograms of FACS after indicated treatments. Representative figures of three distinct experiments are shown by histograms. Overlaid graph of HeLa cells treated with si-*pncRNAD* in addition to si-METTL3, si-YTHDC1, or 0.4 M sorbitol treatment are shown in *light blue histograms*. *C* and *D*, population of each fraction of experiments in *B* were analyzed statistically for siRNA treated cells (*C*) or 0.4 M sorbitol treated cells (*D*). *E*, relative expression level of *CCND1* after siRNA treatments. Expression level of in control cells was set to a value of 1.0 ($n = 3$). *, $p < 0.05$; **, $p < 0.01$; ***, $p < 0.005$.

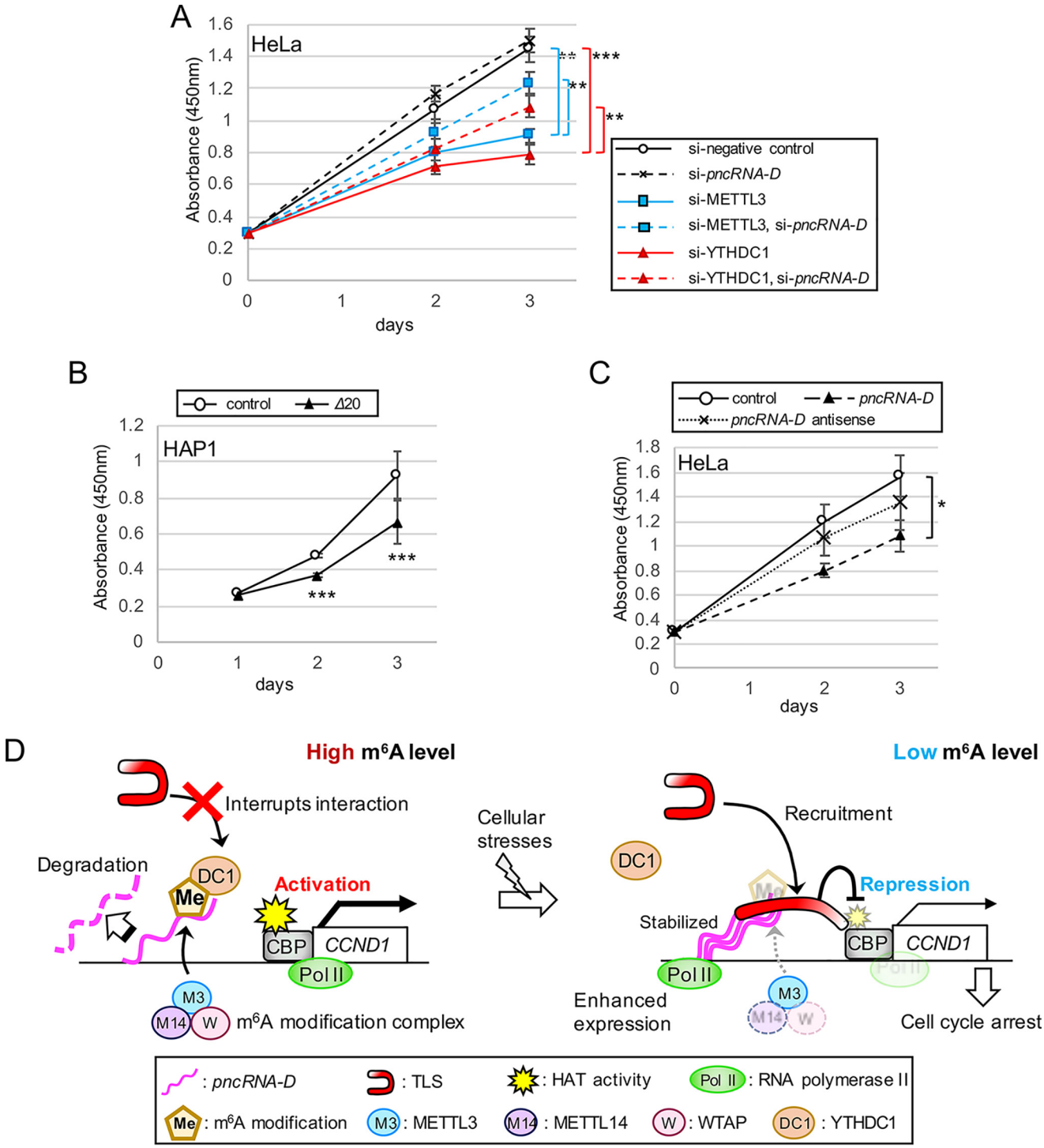

Figure 7. *pncRNA-D* negatively regulates cell proliferation. *A–C*, cell proliferation assay of HeLa cells with indicated siRNA treatments (*A*) or induced RNAs (*C*) or HAP1 cells with or without GGACU deletion (*B*). The numbers of living cells after the indicated number of days after treatments were evaluated. *, $p < 0.05$; **, $p < 0.01$; ***, $p < 0.005$. *D*, model of TLS–*pncRNA-D* inhibitory effect on *CCND1* expression caused by cellular stresses. Normally, *pncRNA-D* is highly methylated, and this modification leads to *pncRNA-D* degradation, and interaction with YTHDC1 inhibits binding to TLS. Therefore, histone acetyltransferase activity of CBP is maintained, and *CCND1* is activated. However, once the cell gets damaged by cellular stresses, *pncRNA-D* expression is enhanced, and decreased methylation stabilizes it and thereafter recruits TLS to the promoter. Interaction with *pncRNA-D* enables TLS to inhibit histone acetyltransferase (*HAT*) activity of CBP and subsequently reduces the expression of *CCND1*, which results in cell cycle arrest.

in regions around 3′ end also supports this speculation (15, 50). Experiments with HAP1 cells lacking the GGACU motif resulted in decreased m^{6}A level and enhanced TLS interaction, but RNA stability was not affected. Because the reduced methylation level destabilized *pncRNA-D*, other RRACH motifs in *pncRNA-D* should be m^{6}A-modified and functions in RNA stabilization. Nevertheless, our data show that m^{6}A modification in *pncRNA-D* could alter its stability and interaction with RNA-binding proteins in HeLa and HAP1 cells.

Sama *et al.* (38) have reported that TLS changes its localization to cytoplasm, especially to stress granules, after 0.4 M sorbitol treatment. We also confirmed that population of nuclear TLS decreased after the osmotic stress, and moreover, the arginine methylation level of TLS in the nucleus was reduced after the treatment. Interestingly, other groups reported that down-regulated arginine methylation by knockdown of PRMT1 reduces cytotoxic TLS cytoplasmic localization (51, 52). In other words, arginine-methylated TLS changes its localization to cytoplasm. Despite the decrease of TLS in the nucleus by osmotic stress, nonmethylated TLS in the nucleus is able to bind *pncRNA-D* and assumed to be enough for *CCND1* repression by *pncRNA-D*. We have previously reported that the methylation of Arg^{476} of TLS inhibits the interaction with RNA (8). The present study demonstrated that *pncRNA-D* m^{6}A modification is decreased by osmotic stress, and both arginine and RNA methylation work negatively in the TLS–RNA interplay. Collectively, we propose that the diverse alteration of RNA and protein methylation in response to osmotic stress regulates RNA–protein interaction.

m^{6}A modification of *pncRNA-D* significantly shortened its half-life. Knockdown of m^{6}A-binding protein YTHDF2 stabilizes mRNAs in cytoplasm (23, 24, 26), but not in the nucleus. The degradation of RNAs in the nucleus is caused by exosome including DGCR8. For example, Hsp70 is degraded by DGCR8 in the nucleus after heat shock (53). Of note, DGCR8 can recognize m^{6}A modification (54), and consequently, *pncRNA-D* could be degraded by DGCR8. Further studies will be required to elucidate the interaction between *pncRNA-D* and DGCR8 and its involvement in *pncRNA-D* degradation.

YTHDC1 is a nuclear RNA-binding protein responsible for RNA splicing (28, 55). However, its function by recognizing m^{6}A of *pncRNA-D* is presumably not splicing, because *pncRNA-D* is a single exon lncRNA. Thus, we predicted that it may alter the binding between *pncRNA-D* and TLS, and the result clearly showed that YTHDC1 could inhibit the interaction. To best of our knowledge, this is the first report that proposes a competitive effect of YTHDC1 on protein–RNA interplay.

Osmotic stress had a similar effect on cell cycle as knockdown of METTL3 or YTHDC1, but the knockdown of *pncRNA-D* in addition to above treatments had different effects. Unlike double knockdown of METTL3 or YTHDC1 with *pncRNA-D*, knockdown of *pncRNA-D* could not rescue the cell cycle arrest at G_0/G_1 phase caused by the osmotic stress. This is because osmotic stress could decrease cyclin D1 protein level directly (56). Therefore, cell cycle arrest could not be rescued by the knockdown of *pncRNA-D*, which was not enough to overcome the effect of cyclin D1 destabilization after osmotic stress. We should note that knockdown of METTL3 or YTHDC1, or osmotic stress might cause cell cycle arrest independent of *pncRNA-D* and *CCND1* by altering expression of other cell cycle–related genes.

In the article in which we demonstrated the TLS–*pncRNA-D* inhibitory system in *CCND1* expression (6), we indicated that *pncRNA-D* principally works in *cis*, but because the exogenous *pncRNA-D* suppressed the proliferation of HeLa cells, there is a possibility that it could also work in *trans*. Several lncRNAs have been reported to work both in *cis* and in *trans* (57, 58), but generally, individual lncRNA regulate different genes in *cis* or in *trans*. However, there is lncRNA such as *ANRIL*, which is able to reduce expression of neighboring gene (*CDKN2B*) both in *cis* and in *trans* (59). We should further validate whether the *pncRNA-D* inhibitory effect is not specific to HeLa cells but could also work in cells derived from other types of cancers. If we could confirm the effect in various cancer-derived cell lines, this sequence could be applied for seed sequence for oligonucleotide therapeutics for suppressor of cancer progression.

In summary, we report the importance of RNA methylation in modestly expressed lncRNA, which controls the stability and interaction with RNA-binding proteins. Our data provide precise regulation of *CCND1* expression by lncRNA and RNA-binding proteins after cellular stresses and also in the normal cell cycle.

Experimental procedures

Cell culture and nuclear extract preparation

HeLa cell culture and nuclear extract preparation were conducted as previously described (9, 60). For nuclear extract with YTHDC1 knockdown HeLa cells, the cells were cultured in a 15-cm dish with 70% confluence, and AllStar negative control siRNA (1027280, Qiagen) or siRNAs targeting YTHDC1 (GGA UGA UAU UUU AAC UGA A, and CAG UAA AGA UCG GAC GUG A) were transfected by RNAiMAX (13778150, Invitrogen) at the final concentration of 10 nM. The cells were cultured for 48 h in 37 °C with 5% CO_2, and the nuclear extract was prepared as above. HAP1 cells (control and TLS-KO cells, HZGHC-001314c002 Horizon) were cultured in Iscove's modified Dulbecco's medium supplemented with 10% FBS and 1× penicillin/streptomycin (PS) (26252-94, Nacalai Tesque). For GFP-TLS overexpression, the TLS coding sequence was cloned into pAcGFP1-C3 vector (632482, Clontech Laboratories) with the primers listed in Table 1, and the plasmid was transfected to TLS-KO HAP1 cells by Lipofectamine 3000 (L3000015, Invitrogen) according to the manufacturer's protocol.

Irradiation, heat shock, osmotic stress, and actinomycin D treatment

Irradiation was treated to HeLa cells as previously described (6). For heat shock, HeLa cells were cultured at 80–90% confluence in 24-well plate and incubated at 43 °C for 30 min. For osmotic stress, HeLa cells were cultured at 80–90% confluence, and the media were exchanged to DMEM, 10% FBS, 1× PS, 0.4 M sorbitol (S3889, Sigma) for 2 h at 37 °C, 5% CO_2. For actinomycin D treatment, the cells were transfected with AllStar negative control siRNA or si-*pncRNA-D* (AAU UCA GUC CCA GGG CAA A and CUG CUU AAG UUU GCG AUA A), si-METTL3 (GCA CAU CCU ACU CUU GUA A and CUG CAA GUA UGU UCA CUA U), or si-YTHDC1 as described above. After 48 h, the media were changed to DMEM, 10% FBS, 1× PS with actinomycin D (00393-41, Nacalai Tesque) at the final

Table 1
Primers used in the study

	Sense	Antisense
RT-qPCR		
pncRNA-D	5′-GGGACCCTCTCATGTAACCA-3′	5′-GAGCCGGCATAATTCAGAAC-3′
GAPDH	5′-CATCACCATCTTCCAGGAGCG-3′	5′-CACCACCTTCTTGATGTCATA-3′
CCND1	5′-CGTGGCCTCTAAGATGAAGG-3′	5′-CTGGCATTTTGGAGAGGAAG-3′
METTL3	5′-CCCTGTCGCAAGCTGCACTT-3′	5′-AACTCCATGGCCCTGCCTGT-3′
METTL14	5′-TTCGACCAGGCTGGCTCACA-3′	5′-AGCCACCTCTGTGTGCTCCT-3′
WTAP	5′-GCAGCTGCTCCATTGTGCCT-3′	5′-TTCCCTGCGTGCAGACTCCT-3′
FTO	5′-ACCGAGTGGCAGAGTGCTCA-3′	5′-CGGGCAATTCGTGACTGGCA-3′
ALKBH5	5′-TCGTCAACAGCGCCGTCATC-3′	5′-AACACGGAGCTGCTCAGGGA-3′
ChIP		
−3 kb control	5′-CAGGGAATCTCTGGTGGATT-3′	5′-GGCGATTCTAATTCCTCGAC-3′
pncRNA-D promoter	5′-GAGGAATTCACCCTGAAAGGTG-3′	5′-CAAACCACCGTACCCTCTTA-3′
CCND1 promoter	5′-AACGTCACACGGACTACAG-3′	5′-ACTCTGCTGCTCGCTGCTAC-3′
CRISPR guide RNA		
pncRNA-D 453–476	5′-CACCGAAATATTAGTCCCCTCTGCC-3′	5′-AAACGGCAGAGGGGACTAATATTTC-3′
Luciferase assay		
pncRNA-D promoter	5′-ATGGTACCCCTCACGCTCACGAATT-3′	5′-ACGAAGCTTGCTCCAGGACTTTGCA-3′
Overexpression		
GFP--TLS	5′-ACCGCTCGAGATGGCCTCAAACGATTATAC-3′	5′-TATACTGCAGCTAATACGGCCTCTCCCTGC-3′
Strep-YTHDC1	5′-AGAATTCAGCGGCTGACAGTCGGGA-3′	5′-GCCCTGCAGTTATCTTCTATATCGA-3′

concentration of 5 μg/ml, and RNA was collected at indicated time point in each experiment.

cDNA preparation and RT-qPCR

Total RNAs were collected by the ReliaPrep RNA cell miniprep system (Z6012, Promega). cDNA was prepared by a PrimeScript RT reagent kit with gDNA Eraser (RR047A, TaKaRa) using 500 ng of total RNAs. RT-qPCR was performed with KOD-SYBR (QKD-201, Toyobo) according to the manufacturer's instructions using the primers listed in Table 1.

ChIP and RIP assay

ChIP assay was conducted by Magna-ChIP kit (17-10085, Millipore) according to the manufacturer's instructions. 5 μg of antibodies for RNA polymerase II (4H8, Thermo Fisher Scientific), TBP (ab818, Abcam), and TFIIB (ab12094, Abcam) were used. RIP assay was performed by Magna-RIP kit (17–700, Millipore) according to the manufacturer's instructions. 5 μg of anti-m^{6}A (202-003, Synaptic Systems), anti-TLS (ab70381, Abcam), anti-YTHDF1 (17479-1-AP, Proteintech), anti-YTHDF2 (24744-1-AP, Proteintech), anti-hnRNP A2B1 (ab6102, Abcam), anti-hnRNP C (ab10294, Abcam), anti-YTHDC1 (A305-096A, Bethyl Laboratories), and anti-normal mouse IgG (CS200621, Millipore) antibodies were used. RNA bound to each protein was collected by phenol/chloroform extraction followed by ethanol precipitation, and RT-qPCR was performed as above with primers listed in Table 1.

RNA pulldown assay and overexpression of GST–TLS and strep-YTHDC1

RNA pulldown assay was performed as previously described (9) with slight modifications. Biotinylated 200-nt RNA fragments used in the assays (Fragments A and m^{6}A) were generated and purchased from Hokkaido System Science. Fragments A or m^{6}A were incubated with GST–TLS and various concentrations of strep-YTHDC1. Overexpression of GST–TLS was performed as previously described (8). For strep-YTHDC1, the coding region was amplified by PrimeSTAR GXL DNA polymerase (R050A, TaKaRa) with primers listed in Table 1, and the fragment was inserted to pASK-IBA5plus vector (2-1404-000, IBA). Overexpression and purification were conducted as previously described (8).

Cell cycle analysis

HeLa cells were transfected with AllStar negative control siRNA, si-*pncRNA-D*, si-METTL3, or si-YTHDC1 for 48 h or treated with 0.4 M sorbitol for 2 h and stained with 10 μg/ml Hoechst 33342 (B2261, Sigma) for 1 h at 37 °C. The cells were then analyzed by cell sorter (SH800Z, SONY). To collect RNAs from the G_0/G_1, S, and G_2/M phase cells, the cells were fractionated by the DNA contents, and total RNA was isolated as described above.

Western blotting analysis

Western blotting analysis was performed as previously described (8) with slight modifications. The antibodies used were anti-METTL3 (15073-1-AP, Proteintech), anti-YTHDC1 (A305-096A, Bethyl Laboratories), anti-mono and di-methylarginine (7E6, ab412, Abcam), and anti-TLS/FUS (611385, BD Biosciences) for primary antibodies at the concentration of 1:2,000, anti-rabbit IgG horseradish peroxidase–linked antibody (7074S, Cell Signaling), and anti-mouse Igs/horseradish peroxidase (P0161, DAKO) for secondary antibodies at the concentration of 1:5,000. The signals were detected by Chemi-Lumi One Super (02230-30, Nacalai Tesque).

Overexpression of pncRNA-D sense and antisense strand

602-nt full-length *pncRNA-D* and antisense *pncRNA-D* was *in vitro* transcribed by a MEGAscript kit (AM1334, Thermo Fisher Scientific) according to the manufacturer's instructions. Briefly, sense and antisense sequence of *pncRNA-D* were inserted to pcDNA 3.1 (+) vector (V790-20, Thermo Fisher Scientific), and RNA was synthesized by T7 transcription.

Cell proliferation assay

HeLa cells were harvested in 96-well plate at 2.5×10^3 cells/well. The next day, the cells were transfected with AllStar negative control siRNA or siRNAs targeting *pncRNA-D*, METTL3, or YTHDC1 by RNAiMAX at the final concentration of 10 nM or induction of 5 pmol sense or antisense strand *pncRNA-D* by JetMessenger (150-001, Polyplus) according to the manufacturer's protocol. Cell proliferation rates were measured by Cell Count Reagent SF (07553-15, Nacalai Tesque) according to the manufacturer's instructions.

Me-RIP-seq data analysis

Me-RIP-seq data by anti-m^{6}A antibody were obtained from GEO accession viewer (GSE46705). Sequence reads were subjected to filtration for quality check by FastQC, the low quality ($Q < 33$) and short reads were excluded, and adapter sequences were removed by fastx_toolkit. Subsequently, the reads were mapped to the human genome (hg18 assembly) using TopHat software.

Lentivirus production for removing GGACU motif in pncRNA-D

The guide RNA targeting *pncRNA-D* GGACU motif was designed by CRISPRdirect (RRID SCR_018186; Table 1), and the specific target sequence was cloned into lenti-CRISPR vectors and verified by DNA sequencing. To produce lentivirus, HEK 293FT cells seeded in 10-cm plates were transfected with 6 μg of lenti-CRISPR-v2 (52961, Addgene), 4 μg of psPAX2 (12260, Addgene), and 3 μg of pLP-VSVG (Invitrogen) plasmids using Lipofectamine 2000 (11668027, Invitrogen) according to the manufacturer's protocol. HEK 293FT cells were cultured for 24 h in DMEM, 10% FBS, 1× PS, and the media were exchanged to Iscove's modified Dulbecco's medium, 10% FBS. After 24 h of culture, the supernatant containing lentivirus was collected, and HAP1 cells were infected with the generated lentiviruses in the presence of 8 μg/ml Polybrene and selected with 1 μg/ml puromycin for 6 days. The cells were collected, and a single cell per well was seeded in a 96-well plate by cell sorter. The genome sequence of each clone was examined, and two clones lacking the GGACU motif (Δ20 and Δ46) were obtained.

Luciferase reporter assay

CCND1 promoter regions of control or GGACT removed HAP1 cells (Δ20 and Δ46) were cloned into pGL4.10[luc2] vector (E6651, Promega) with the primers listed in Table 1. 50 ng of empty vector or the above constructs, and 50 ng of *Renilla* luciferase plasmid (pRL-TK, E2241, Promega) were transfected by Lipofectamine 3000 (Invitrogen) into HAP1 cells seeded in a 96-well plate, according to the manufacturer's protocol. The cells were cultured in 37 °C, 5% CO_2 and lysed 48 h after transfection, and luciferase activity was measured using the Dual-Luciferase assay kit (E1910, Promega). Luciferase activities were normalized to *Renilla* luciferase activities.

Statistical analysis

The data are presented as means ± standard deviations. Pairwise differences were identified using two-tailed Student *t* test and were considered significant when $p < 0.05$.

Author contributions—R. Y. funding acquisition; R. Y. investigation; R. Y., N. U., K. U., and M. H. methodology; R. Y. writing-original draft; R. Y., N. U., and R. K. writing-review and editing; R. K. supervision; R. K. project administration.

References

1. Kornfeld, J.-W., and Brüning, J. C. (2014) Regulation of metabolism by long, non-coding RNAs. *Front. Genet.* **5,** 57 Medline
2. Kitagawa, M., Kitagawa, K., Kotake, Y., Niida, H., and Ohhata, T. (2013) Cell cycle regulation by long non-coding RNAs. *Cell Mol. Life Sci.* **70,** 4785–4794 CrossRef Medline
3. Han, Y., Yang, Y.-N., Yuan, H.-H., Zhang, T.-T., Sui, H., Wei, X.-L., Liu, L., Huang, P., Zhang, W.-J., and Bai, Y.-X. (2014) UCA1, a long non-coding RNA up-regulated in colorectal cancer influences cell proliferation, apoptosis and cell cycle distribution. *Pathology* **46,** 396–401 Medline
4. Qin, R., Chen, Z., Ding, Y., Hao, J., Hu, J., and Guo, F. (2013) Long non-coding RNA MEG3 inhibits the proliferation of cervical carcinoma cells through the induction of cell cycle arrest and apoptosis. *Neoplasma* **60,** 486–492 CrossRef Medline
5. Liu, Y., Zhao, J., Zhang, W., Gan, J., Hu, C., Huang, G., and Zhang, Y. (2015) lncRNA GAS5 enhances G_1 cell cycle arrest via binding to YBX1 to regulate p21 expression in stomach cancer. *Sci. Rep.* **5,** 10159 CrossRef Medline
6. Wang, X., Arai, S., Song, X., Reichart, D., Du, K., Pascual, G., Tempst, P., Rosenfeld, M. G., Glass, C. K., and Kurokawa, R. (2008) Induced ncRNAs allosterically modify RNA-binding proteins in *cis* to inhibit transcription. *Nature* **454,** 126–130 CrossRef Medline
7. Yoneda, R., Satoh, Y., Yoshida, I., Kawamura, S., Kotani, T., and Kimura, A. P. (2016) A genomic region transcribed into a long noncoding RNA interacts with the Prss42/Tessp-2 promoter in spermatocytes during mouse spermatogenesis, and its flanking sequences can function as enhancers. *Mol. Reprod. Dev.* **83,** 541–557 CrossRef Medline
8. Cui, W., Yoneda, R., Ueda, N., and Kurokawa, R. (2018) Arginine methylation of translocated in liposarcoma (TLS) inhibits its binding to long noncoding RNA, abrogating TLS-mediated repression of CBP/p300 activity. *J. Biol. Chem.* **293,** 10937–10948 CrossRef Medline
9. Yoneda, R., Suzuki, S., Mashima, T., Kondo, K., Nagata, T., Katahira, M., and Kurokawa, R. (2016) The binding specificity of Translocated in Lipo-Sarcoma/FUsed in Sarcoma with lncRNA transcribed from the promoter region of cyclin D1. *Cell Biosci.* **6,** 4 CrossRef Medline
10. Sun, F., Fu, H., Liu, Q., Tie, Y., Zhu, J., Xing, R., Sun, Z., and Zheng, X. (2008) Downregulation of CCND1 and CDK6 by miR-34a induces cell cycle arrest. *FEBS Lett.* **582,** 1564–1568 CrossRef Medline
11. Baldin, V., Lukas, J., Marcote, M. J., Pagano, M., and Draetta, G. (1993) Cyclin D1 is a nuclear protein required for cell cycle progression in G_1. *Genes Dev.* **7,** 812–821 CrossRef Medline
12. Cantara, W. A., Crain, P. F., Rozenski, J., McCloskey, J. A., Harris, K. A., Zhang, X., Vendeix, F. A., Fabris, D., and Agris, P. F. (2011) The RNA modification database, RNAMDB: 2011 update. *Nucleic Acids Res.* **39,** D195–D201 CrossRef Medline
13. Liu, N., Parisien, M., Dai, Q., Zheng, G., He, C., and Pan, T. (2013) Probing N^6-methyladenosine RNA modification status at single nucleotide resolution in mRNA and long noncoding RNA. *RNA* **19,** 1848–1856 CrossRef Medline
14. Cao, G., Li, H.-B., Yin, Z., and Flavell, R. A. (2016) Recent advances in dynamic m^{6}A RNA modification. *Open Biol.* **6,** 160003 CrossRef Medline
15. Batista, P. J., Molinie, B., Wang, J., Qu, K., Zhang, J., Li, L., Bouley, D. M., Lujan, E., Haddad, B., Daneshvar, K., Carter, A. C., Flynn, R. A., Zhou, C., Lim, K.-S., Dedon, P., *et al.* (2014) m6A RNA modification controls cell

fate transition in mammalian embryonic stem cells. *Cell Stem Cell* **15,** 707–719 CrossRef Medline

16. Schöller, E., Weichmann, F., Treiber, T., Ringle, S., Treiber, N., Flatley, A., Feederle, R., Bruckmann, A., and Meister, G. (2018) Interactions, localization, and phosphorylation of the m6A generating METTL3–METTL14–WTAP complex. *RNA.* **24,** 499–512 CrossRef Medline
17. Lin, Z., Hsu, P. J., Xing, X., Fang, J., Lu, Z., Zou, Q., Zhang, K.-J., Zhang, X., Zhou, Y., Zhang, T., Zhang, Y., Song, W., Jia, G., Yang, X., He, C., *et al.* (2017) Mettl3-/Mettl14-mediated mRNA N^6-methyladenosine modulates murine spermatogenesis. *Cell Res.* **27,** 1216–1230 CrossRef Medline
18. Liu, J., Yue, Y., Han, D., Wang, X., Fu, Y., Zhang, L., Jia, G., Yu, M., Lu, Z., Deng, X., Dai, Q., Chen, W., and He, C. (2014) A METTL3–METTL14 complex mediates mammalian nuclear RNA N^6-adenosine methylation. *Nat. Chem. Biol.* **10,** 93–95 CrossRef Medline
19. Zhao, X., Yang, Y., Sun, B.-F., Shi, Y., Yang, X., Xiao, W., Hao, Y.-J., Ping, X.-L., Chen, Y.-S., Wang, W.-J., Jin, K.-X., Wang, X., Huang, C.-M., Fu, Y., Ge, X.-M., *et al.* (2014) FTO-dependent demethylation of N^6-methyladenosine regulates mRNA splicing and is required for adipogenesis. *Cell Res.* **24,** 1403–1419 CrossRef Medline
20. Zou, S., Toh, J. D., Wong, K. H. Q., Gao, Y.-G., Hong, W., and Woon, E. C. (2016) N^6-Methyladenosine: a conformational marker that regulates the substrate specificity of human demethylases FTO and ALKBH5. *Sci. Rep.* **6,** 25677 CrossRef Medline
21. Liao, S., Sun, H., and Xu, C. (2018) YTH domain: a family of N^6-methyladenosine (m6A) readers. *Genomics Proteomics Bioinformatics* **16,** 99–107 CrossRef Medline
22. Zhao, B. S., Roundtree, I. A., and He, C. (2017) Post-transcriptional gene regulation by mRNA modifications. *Nat. Rev. Mol. Cell Biol.* **18,** 31–42 CrossRef Medline
23. Wang, X., Zhao, B. S., Roundtree, I. A., Lu, Z., Han, D., Ma, H., Weng, X., Chen, K., Shi, H., and He, C. (2015) N^6-Methyladenosine modulates messenger RNA translation efficiency. *Cell* **161,** 1388–1399 CrossRef Medline
24. Ivanova, I., Much, C., Di Giacomo, M., Azzi, C., Morgan, M., Moreira, P. N., Monahan, J., Carrieri, C., Enright, A. J., and O'Carroll, D. (2017) The RNA m^{6}A reader YTHDF2 is essential for the post-transcriptional regulation of the maternal transcriptome and oocyte competence. *Mol. Cell* **67,** 1059–1067.e4 CrossRef Medline
25. Chen, M., Wei, L., Law, C.-T., Tsang, F. H.-C., Shen, J., Cheng, C. L.-H., Tsang, L.-H., Ho, D. W.-H., Chiu, D. K.-C., Lee, J. M.-F., Wong, C. C.-L., Ng, I. O.-L., and Wong, C.-M. (2018) RNA N^6-methyladenosine methyltransferase-like 3 promotes liver cancer progression through YTHDF2-dependent posttranscriptional silencing of SOCS2. *Hepatology* **67,** 2254–2270 CrossRef Medline
26. Du, H., Zhao, Y., He, J., Zhang, Y., Xi, H., Liu, M., Ma, J., and Wu, L. (2016) YTHDF2 destabilizes m^{6}A-containing RNA through direct recruitment of the CCR4-NOT deadenylase complex. *Nat. Commun.* **7,** 12626 CrossRef Medline
27. Lesbirel, S., Viphakone, N., Parker, M., Parker, J., Heath, C., Sudbery, I., and Wilson, S. A. (2018) The m^{6}A-methylase complex recruits TREX and regulates mRNA export. *Sci. Rep.* **8,** 13827 CrossRef Medline
28. Xiao, W., Adhikari, S., Dahal, U., Chen, Y.-S., Hao, Y.-J., Sun, B.-F., Sun, H.-Y., Li, A., Ping, X.-L., Lai, W.-Y., Wang, X., Ma, H.-L., Huang, C.-M., Yang, Y., Huang, N., *et al.* (2016) Nuclear m^{6}A Reader YTHDC1 Regulates mRNA Splicing. *Mol. Cell* **61,** 507–519 CrossRef Medline
29. Kasowitz, S. D., Ma, J., Anderson, S. J., Leu, N. A., Xu, Y., Gregory, B. D., Schultz, R. M., and Wang, P. J. (2018) Nuclear m^{6}A reader YTHDC1 regulates alternative polyadenylation and splicing during mouse oocyte development. *PLoS Genet.* **14,** e1007412 CrossRef Medline
30. Jaffrey, S. R., and Kharas, M. G. (2017) Emerging links between m^{6}A and misregulated mRNA methylation in cancer. *Genome Med.* **9,** 2 CrossRef Medline
31. Patil, D. P., Chen, C.-K., Pickering, B. F., Chow, A., Jackson, C., Guttman, M., and Jaffrey, S. R. (2016) m^{6}A RNA methylation promotes XIST-mediated transcriptional repression. *Nature* **537,** 369–373 CrossRef Medline
32. Fustin, J.-M., Doi, M., Yamaguchi, Y., Hida, H., Nishimura, S., Yoshida, M., Isagawa, T., Morioka, M. S., Kakeya, H., Manabe, I., and Okamura, H. (2013) RNA-methylation–dependent RNA processing controls the speed of the circadian clock. *Cell* **155,** 793–806 CrossRef Medline
33. Wu, R., Liu, Y., Yao, Y., Zhao, Y., Bi, Z., Jiang, Q., Liu, Q., Cai, M., Wang, F., Wang, Y., and Wang, X. (2018) FTO regulates adipogenesis by controlling cell cycle progression via m^{6}A-YTHDF2 dependent mechanism. *Biochim. Biophys. Acta Mol. Cell Biol. Lipids.* **1863,** 1323–1330 CrossRef Medline
34. Li, X., Tang, J., Huang, W., Wang, F., Li, P., Qin, C., Qin, Z., Zou, Q., Wei, J., Hua, L., Yang, H., and Wang, Z. (2017) The m^{6}A methyltransferase METTL3: acting as a tumor suppressor in renal cell carcinoma. *Oncotarget* **8,** 96103–96116 Medline
35. Horiuchi, K., Kawamura, T., Iwanari, H., Ohashi, R., Naito, M., Kodama, T., and Hamakubo, T. (2013) Identification of Wilms' tumor 1–associating protein complex and its role in alternative splicing and the cell cycle. *J. Biol. Chem.* **288,** 33292–33302 CrossRef Medline
36. Shima, H., Matsumoto, M., Ishigami, Y., Ebina, M., Muto, A., Sato, Y., Kumagai, S., Ochiai, K., Suzuki, T., and Igarashi, K. (2017) *S*-Adenosylmethionine synthesis is regulated by selective N^6-adenosine methylation and mRNA degradation involving METTL16 and YTHDC1. *Cell Rep.* **21,** 3354–3363 CrossRef Medline
37. Shi, X., Sun, M., Liu, H., Yao, Y., and Song, Y. (2013) Long non-coding RNAs: a new frontier in the study of human diseases. *Cancer Lett.* **339,** 159–166 CrossRef Medline
38. Sama, R. R., Ward, C. L., Kaushansky, L. J., Lemay, N., Ishigaki, S., Urano, F., and Bosco, D. A. (2013) FUS/TLS assembles into stress granules and is a prosurvival factor during hyperosmolar stress. *J. Cell Physiol.* **228,** 2222–2231 CrossRef Medline
39. Wang, X., Lu, Z., Gomez, A., Hon, G. C., Yue, Y., Han, D., Fu, Y., Parisien, M., Dai, Q., Jia, G., Ren, B., Pan, T., and He, C. (2014) N^6-methyladenosine-dependent regulation of messenger RNA stability. *Nature* **505,** 117–120 CrossRef Medline
40. Schwartz, S., Mumbach, M. R., Jovanovic, M., Wang, T., Maciag, K., Bushkin, G. G., Mertins, P., Ter-Ovanesyan, D., Habib, N., Cacchiarelli, D., Sanjana, N. E., Freinkman, E., Pacold, M. E., Satija, R., Mikkelsen, T. S., *et al.* (2014) Perturbation of m^{6}A writers reveals two distinct classes of mRNA methylation at internal and 5′ sites. *Cell Rep.* **8,** 284–296 CrossRef Medline
41. Chen, K., Lu, Z., Wang, X., Fu, Y., Luo, G.-Z., Liu, N., Han, D., Dominissini, D., Dai, Q., Pan, T., and He, C. (2015) High-resolution N^6-methyladenosine (m^{6}A) map using photo-crosslinking-assisted m^{6}A sequencing. *Angew. Chem. Int. Ed. Engl.* **54,** 1587–1590 CrossRef Medline
42. Śledź;, P, and Jinek, M. (2016) Structural insights into the molecular mechanism of the m^{6}A writer complex. *Elife* **5,** e18434 CrossRef Medline
43. Visvanathan, A., and Somasundaram, K. (2018) mRNA traffic control reviewed: N^6-methyladenosine (m^{6}A) takes the driver's seat. *BioEssays* **40,** 1700093 CrossRefMedline
44. Zhang, S., Zhao, B. S., Zhou, A., Lin, K., Zheng, S., Lu, Z., Chen, Y., Sulman, E. P., Xie, K., Bögler, O., Majumder, S., He, C., and Huang, S. (2017) m^{6}A demethylase ALKBH5 maintains tumorigenicity of glioblastoma stem-like cells by sustaining FOXM1 expression and cell proliferation program. *Cancer Cell* **31,** 591–606.e6 CrossRef Medline
45. Vilborg, A., Passarelli, M. C., Yario, T. A., Tycowski, K. T., and Steitz, J. A. (2015) Widespread inducible transcription downstream of human genes. *Mol. Cell* **59,** 449–461 CrossRef Medline
46. Leong, H. S., Dawson, K., Wirth, C., Li, Y., Connolly, Y., Smith, D. L., Wilkinson, C. R., and Miller, C. J. (2014) A global non-coding RNA system modulates fission yeast protein levels in response to stress. *Nat. Commun.* **5,** 3947 CrossRef Medline
47. Waldman, T., Kinzler, K. W., and Vogelstein, B. (1995) p21 is necessary for the p53-mediated G_1 arrest in human cancer cells. *Cancer Res.* **55,** 5187–5190 Medline
48. Narayanan, B. A., Geoffroy, O., Willingham, M. C., Re, G. G., and Nixon, D. W. (1999) p53/p21(WAF1/CIP1) expression and its possible role in G_1 arrest and apoptosis in ellagic acid treated cancer cells. *Cancer Lett.* **136,** 215–221 CrossRef Medline
49. Palombo, R., Frisone, P., Fidaleo, M., Mercatelli, N., Sette, C., and Paronetto, M. P. (2019) The promoter associated non-coding RNA pncCCND1_B assembles a protein–RNA complex to regulate cyclin D1

transcription in Ewing sarcoma. *Cancer Res.* **79,** 3570–3582 CrossRef Medline

50. Ke, S., Alemu, E. A., Mertens, C., Gantman, E. C., Fak, J. J., Mele, A., Haripal, B., Zucker-Scharff, I., Moore, M. J., Park, C. Y., Vågbø, C. B., Kusśnierczyk, A., Klungland, A., Darnell, J. E., Jr., and Darnell, R. B. (2015) A majority of m^{6}A residues are in the last exons, allowing the potential for 3′ UTR regulation. *Genes Dev.* **29,** 2037–2053 CrossRef Medline
51. Yamaguchi, A., and Kitajo, K. (2012) The effect of PRMT1-mediated arginine methylation on the subcellular localization, stress granules, and detergent-insoluble aggregates of FUS/TLS. *PLoS One* **7,** e49267 CrossRef Medline
52. Tradewell, M. L., Yu, Z., Tibshirani, M., Boulanger, M.-C., Durham, H. D., and Richard, S. (2012) Arginine methylation by PRMT1 regulates nuclear-cytoplasmic localization and toxicity of FUS/TLS harbouring ALS-linked mutations. *Hum. Mol. Genet.* **21,** 136–149 CrossRef Medline
53. Knuckles, P., Carl, S. H., Musheev, M., Niehrs, C., Wenger, A., and Bühler, M. (2017) RNA fate determination through cotranscriptional adenosine methylation and microprocessor binding. *Nat. Struct. Mol. Biol.* **24,** 561–569 CrossRef Medline
54. Widagdo, J., and Anggono, V. (2018) The m^{6}A-epitranscriptomic signature in neurobiology: from neurodevelopment to brain plasticity. *J. Neurochem.* **147,** 137–152 CrossRef Medline
55. Zhang, Z., Theler, D., Kaminska, K. H., Hiller, M., de la Grange, P., Pudimat, R., Rafalska, I., Heinrich, B., Bujnicki, J. M., Allain, F. H., and Stamm, S. (2010) The YTH domain is a novel RNA binding domain. *J. Biol. Chem.* **285,** 14701–14710 CrossRef Medline
56. Casanovas, O., Miró, F., Estanyol, J. M., Itarte, E., Agell, N., and Bachs, O. (2000) Osmotic stress regulates the stability of cyclin D1 in a p38SAPK2-dependent manner. *J. Biol. Chem.* **275,** 35091–35097 CrossRef Medline
57. Guil, S., and Esteller, M. (2012) *cis*-Acting noncoding RNAs: friends and foes. *Nat. Struct. Mol. Biol.* **19,** 1068–1075 CrossRef Medline
58. Hitachi, K., Nakatani, M., Takasaki, A., Ouchi, Y., Uezumi, A., Ageta, H., Inagaki, H., Kurahashi, H., and Tsuchida, K. (2019) *Myogenin* promoter-associated lnc RNA *Myoparr* is essential for myogenic differentiation. *EMBO Rep.* **20,** e47468 Medline
59. Yu, W., Gius, D., Onyango, P., Muldoon-Jacobs, K., Karp, J., Feinberg, A. P., and Cui, H. (2008) Epigenetic silencing of tumour suppressor gene p15 by its antisense RNA. *Nature* **451,** 202–206 CrossRef Medline
60. Fujimoto, K., and Kurokawa, R. (2014) Development of a mouse monoclonal antibody for the detection of asymmetric dimethylarginine of Translocated in LipoSarcoma/FUsed in Sarcoma and its application in analyzing methylated TLS. *Cell Biosci.* **4,** 77 CrossRef Medline